S-72.333

Postgraduate Course in Radio Communications
Spring 2004

WLAN radio channel modelling
17.2.2004

Aki Silvennoinen, 46927U
Aki.Silvennoinen@hut.fi

Table of contents

1. Introduction

The development of WLAN systems is leading towards higher and higher transferred data rates, which are using more and more complex modulation methods. Complex modulation methods make the systems more sensitive to interference particularly intersymbolic interference (ISI) caused by multipath propagation. Therefore, there is a great need for detailed radio channel information to be able to understand and compensate communication quality degradation by countermeasures.

IEEE 802.11b WLAN system operates in the license-free 2.4 GHz frequency band. Due to the popularity of IEEE 802.11b, the 2.4 GHz frequency band has been researched quite a lot. The channel characteristics in indoor and urban city environments are quite well known and different channel modelling results are available in the books and scientific journals. Urban or sub-urban outdoor environments display different propagation conditions due e.g. vegetation, large delay spreads and perhaps fewer multipath components.

This seminar paper presents WLAN radio channel modelling concepts, radio wave propagation and existing channel models for various environments as an overview to the subject. Chapter 2 inspects basic radio wave propagation mechanisms. These mechanisms are the basics upon which more complicated channel models are being developed. In Chapter 3, suitable existing channel models are presented. The focus is on outdoor environments and on propagation in vegetation. Large-scale models include distance path loss and shadowing loss models, whereas small-scale models are more accurate and based on system functions of linear time-variant channel.

2. Radio wave propagation

Radio wave propagation plays a significant role in the performance of radio systems. Radio waves, i.e. electromagnetic waves, propagate in a radio channel that is understood as the radio path between the transmitter and the receiver, including antennas. The radio path consists of a variable environment and various obstacles that affect the way the radio waves propagate.

Radio wave propagation could be modelled exactly by using Maxwell's equations for electromagnetic field theory, but this method would be mathematically restrictively complex and is therefore not included in this paper.

Fixed radio systems (e.g. terrestrial radio relay systems) are planned in such a way that there are no obstacles that cause attenuation in the radio path. This is called line-of-sight (LOS) situation. LOS situation is often impossible to maintain while using mobile radio systems, e.g. WLAN, since these are many times used in an urban environment. In such environments there are usually many objects and reflecting surfaces in the radio path that affect the radio wave propagation.

Therefore such a situation is called non-line-of-sight (NLOS).

There are four basic phenomena that are understood as the basic radio wave propagation mechanisms in this paper: free space loss, reflection and penetration, diffraction, and scattering. They are introduced in Section 2.1.

2.1. Physical propagation mechanisms

The radio path may consist of various obstacles which affect the radio wave propagation. The radio wave can be reflected from the surface of the obstacle and it can penetrate into it. Large obstacles can cause scattering and edges of the obstacles can diffract the signal to various directions. Each of these events attenuates the signal.

2.1.1. Free space loss

The most simple radio wave propagation mechanism is free space propagation. It is assumed that there are no obstacles or reflecting surfaces in the radio path between transmitter and receiver. It is also assumed that antennas are separated so they are not located in the near field of each other. Under these assumptions there is no multipath propagation and the wave is not absorbed. Since there are also no reflections, the received power level can be calculated directly as a function of distance between antennas if the transmitted power is known. The power density within a region with a certain radius is proportional to the area where the power is spread. The transmitted radiation in a certain direction is described by antenna gain and transmitted power P_{TX}. The power is spread spherically. Thus, at distance r the power density S_d is given by (1) [Lin96, p.8]:

$$S_d = \frac{G_{TX} P_{TX}}{4\pi r^2} \qquad (1)$$

The receiving antenna intercepts this power density using a cross section A_e that is defined as a function of antenna gain G_{RX} and wavelength λ, as shown in (2) [Lin96, p.8]:

$$A_e = \frac{\lambda^2}{4\pi} G_{RX} \qquad (2)$$

Therefore, the received power can be calculated by using (3) [Lin96, p.8]:

$$P_{RX} = A_e S_d = G_{TX} G_{RX} P_{TX} \left(\frac{\lambda}{4\pi r} \right)^2, \qquad (3)$$

where the term $\left(\lambda/4\pi r \right)^2$ is the actual free space loss, which is normally denoted as L_0. In many cases the free space loss is given in dB as in (4):

$$L_0 = 32.45 + 20\log f_{[MHz]} + 20\log r_{[km]} \qquad (4)$$

2.1.2. Reflection and penetration

When the radio wave hits a surface large enough in comparison with its wavelength, part of its power is reflected from the surface and part of it penetrates through the surface. The dimensions of the reflection surface are defined by a Fresnel's zone that is discussed in Section 2.1.3.

The reflection angle of the radio wave is the same as the incidence angle ϕ_1. The reflection loss depends on the electrical properties of the medium on both sides of the reflecting surface, the frequency used, the incidence angle and the polarization of the radio wave. Figure 1 presents the reflection of both polarisations: perpendicular and parallel [Lin96, p.46]. Parallel polarisation states that magnetic field H is parallel to the plane of incidence, whereas perpendicular polarisation states that electric field E is parallel to the plane of the incidence. Parallel polarisation is also referred to as vertical polarisation (or TM) and perpendicular polarisation is referred to as horizontal polarisation (or TE).
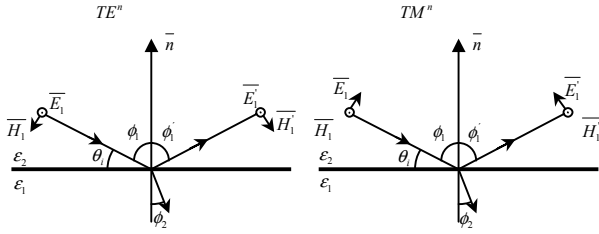

Figure 1 Reflection of perpendicular and parallel-polarised plane wave.

The Fresnel reflection coefficients for perpendicular and parallel polarisation, $\Gamma_\perp$ and $\Gamma_\parallel$, respectively, are presented in (5) and (6) [Lin96, p.47].

$$\Gamma_\perp = \frac{\sin\theta_i - \sqrt{\varepsilon - \cos^2\theta_i}}{\sin\theta_i + \sqrt{\varepsilon - \cos^2\theta_i}} \qquad (5)$$

$$\Gamma_\parallel = \frac{\varepsilon\sin\theta_i - \sqrt{\varepsilon - \cos^2\theta_i}}{\varepsilon\sin\theta_i + \sqrt{\varepsilon - \cos^2\theta_i}}, \qquad (6)$$

where $\varepsilon = \varepsilon_1/\varepsilon_2$ is the relative permittivity of the materials.

The reflection coefficients depend on the surface of reflection, and equations (5) and (6) are based on the ideal situation. If the surface is spherical or unsmooth there is an additional reduction in the reflection coefficients. In reality the reflections occur usually in urban environments, where the radio wave is reflected from the surface of the earth, walls, cars or other obstacles that are not ideal. Therefore exact modelling of the propagation channel can become very complex.

The part of the radio wave that is not reflected penetrates into inside the surface material. Penetration coefficients for perpendicular and parallel polarisation, $T_\perp$ and $T_\parallel$, respectively, are given in (7) and (8) [Nik92, p.69].

$$T_\perp = 1 + \Gamma_\perp \qquad (7)$$

$$T_\parallel = \left(1 + \Gamma_\parallel\right)\frac{\cos\phi_1}{\cos\phi_2}, \qquad (8)$$

where $\phi_1 = \pi/2 - \gamma$ and ϕ_2 can be calculated using Snell's law (9) [Nik92, p.70] as a function of incidence angle, permittivity and permeability of the material, $\varepsilon_{1,2}$ and $\mu_{1,2}$, respectively.

$$\sqrt{\mu_1\varepsilon_1}\sin\varphi_1 = \sqrt{\mu_2\varepsilon_2}\sin\varphi_2 \qquad (9)$$

2.1.3. Diffraction

According to Huyghen's principle almost all of the transmitter power propagates within the 1st Fresnel zone. If it is kept clear of obstacles, the radio wave propagates according to the free space propagation principle. If there is an obstacle partly covering the zone, the signal is attenuated. The signal also bends behind the obstacle and this phenomenon is called diffraction. In particular, with diffraction there is still the possibility of receiving the radio signal even without any reflecting surfaces and when there is no line-of-sight between TX and RX.

The radius of the 1st Fresnel zone is calculated with using (10) [Lin96, p.29].

$$b = \sqrt{\frac{\lambda d_1 d_2}{d_1 + d_2}}, \qquad (10)$$

where λ is wavelength and $d_{1,2}$ are distances between antenna and obstacle as shown in Figure 2.
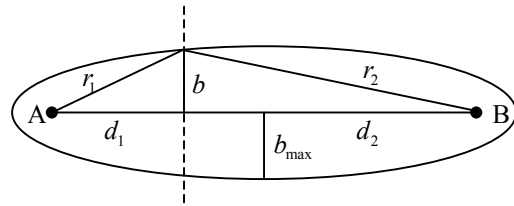
Figure 2 Fresnel zone.

The radius is at maximum, when the obstacle is at the centre of the node, as in (11).

$$d_1 = d_2 = 0.5d$$
$$\Rightarrow b_{max} = \frac{\sqrt{\lambda d}}{2} \qquad (11)$$

An obstacle penetrating into the 1st Fresnel zone causes attenuation that can be estimated according to the shape of the obstacle. Knife-edge diffraction (Figure 3) is referred to when the obstacle is assumed to be an

indefinitely thin plate. The attenuation can be approximated according to (12) [Lin96, p.36].

$$F \approx 0.452 \left(\sqrt{(v-0.1)^2 + 1} - (v - 0.1) \right), \quad (12)$$

where v depends of the height H of the obstacle, as in (13).
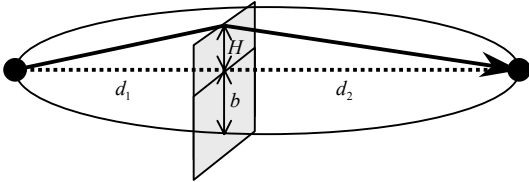
$$v = \sqrt{2} \frac{H}{b} \qquad (13)$$

Figure 3 Knife-edge diffraction.

Naturally, all objects that cause diffraction are not sharp. Hills and other rounded objects can cause rounded obstacle diffraction loss that is greater that knife-edge diffraction, and objects that are shaped like wedges or corners cause a different kind of diffraction.

2.1.4.   Scattering

Scattering propagation is referred to, when an obstacle or particle with dimensions that are small related to the wavelength, alters the radio wave propagation by retransmitting the signal in various directions. If there are a large amount of particles, a substantial amount of transmitter power can be lost. However, scattering can also help transmission by reflecting the radio wave behind shadows or obstacles to positions that are normally out of reach of the radio system. Also, in multipath environments, scattering can strengthen the received signal since new multipath channels are formed by the scattering elements. However, scattering causes polarisation cross coupling and therefore the received signal might not have the same polarisation as the transmitted signal. At high frequencies, atmospheric gases and rain cause scattering losses to signals.
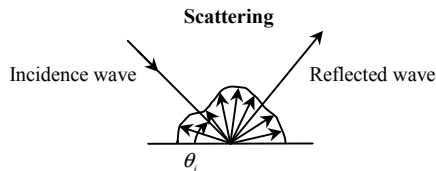

Figure 4 Scattering caused by unsmooth surface.

Reflection from an unsmooth surface causes scattering as shown in Figure 4. The power scattered from an unsmooth surface can be calculated by using (14) [Rap96, p.101][Ame53, p.145]

$$\rho_s = e^{\left[-8 \left(\frac{\pi \cdot \sigma_h \cdot \sin \theta_i}{\lambda} \right)^2 \right]}, \qquad (14)$$

where θ_i is the angle of incidence and σ_h is the standard deviation of the surface height about the mean surface height. It is assumed that the surface height is a Gaussian distributed random variable. Existing channel models

3. Channel models

Various radio wave propagation channel models have been developed to estimate the path attenuation, or other parameters of the propagation channel. There are variations in calculation methods, initial values, and results between different models.

Channel models can be categorised in many ways, for instance according to how they are created. Empirical models are based on statistical analysis of a large amount of measurements. Usually the simplest models estimate the path loss with the aid of a set of diagrams that are based on empirical measurements. These models can be scaled to a certain environment using simple parameters such as antenna heights. COST231 Hata-model (European Co-operation in the field of Scientific and Technical Research, action 231) is an example of such a model. It uses frequency, distance between TX and RX, and antenna heights as initial parameters. The environment is also characterised by selecting the environment type from dense city, city, suburban or rural environment.

Semi-deterministic models are more complex and based on theoretical calculations and statistics in addition to empirical measurements. The environmental impacts can be modelled more accurately by adding some theoretical aspect to the models. Therefore, these models require extra parameters to characterise the environment. This leads to the situation where the channel models are more environment-specific and need to be recalculated if the conditions change. COST231 Walfisch-Ikegami model is probably the most familiar semi-deterministic channel model for an urban environment. It uses additional parameters, such as building height, street width, block size and direction of the streets.

Deterministic models are based on electromagnetic simulation of the environments. They try to estimate all the characteristics of the radio channel including delays, polarisations and directions of the multipath components. They are based on 3-dimensional maps of the environment and require heavy calculations in order to model the radio channel thoroughly. Deterministic channel models are environment-dependent, and it is hard (or impossible) to find a model that would suit all environments. Finite difference time-domain (FDTD) methods, used for deriving the impulse response, and Ray-tracing approach, where dominant propagation paths are

predicted, are well-known methods to create deterministic channel models.

Radio wave propagation channels can also be divided according to the effects of the channel on the transmitted signal. Traditionally, propagation models have focused on giving estimations for average received signal strength at a certain distance from the transmitter. These simple models are used to estimate the path loss of the radio channel, and are called large-scale propagation models. On the other hand, propagation models that characterise rapid changes of the signal strength over very short distances (a few wavelengths) between TX and RX or short durations (in the order of seconds), are called small-scale or fading models. Examples of large-scale and small-scale models are presented in Sections 3.1 and 3.2, respectively.

3.1. Large-scale propagation models

Propagation models that estimate the mean signal strength for different distances between TX and RX in the order of several hundreds or thousands of meters are called large-scale propagation models. Large-scale models are quite simple and do not take in account very small variations e.g. fading caused by multipath propagation. These models are useful e.g. in predicting coverage of a radio system.

Many models that are found in the literature are created for estimating the propagation losses in a macrocell environment using frequencies below 2 GHz. These models can be created for various environments, e.g. COST231 Hata model for rural, suburban and urban environments and COST231 Walfisch-Ikegami model for urban environments. Nevertheless, modern radio systems use higher frequencies or demand higher capacity, and therefore the cell size is decreasing. For instance, outdoor WLAN systems operate above 2 GHz and mainly in microcells. Therefore, efforts have also been directed towards studying microcell propagation above 2 GHz, and channel models can be found especially for city environment e.g. Har-Xia-Bertoni model for microcell city environment [Har99a]. These models take into account the street-guided wave, which is a distinct characteristic of microcells. However, according to Parsons, the models that exist at present are only valid in flat urban areas and the effects of terrain variations or vegetation are largely ignored [Par00, p.108]. ITU-R Recommendation P.833 offers a method for take account the effect of vegetation.

Large-scale fading models typically include path loss over distance and shadowing models. In this section, various channel models for various environments are presented, while the emphasis is on models suitable for WLAN usage. Sections 3.1.1 to 3.1.3 consider the path loss channel models, and Section 3.1.4 deals with the shadowing model.

3.1.1. Log-distance path loss model

Theoretical analysis and measurements have indicated that the average received signal power decreases logarithmically over distance in both indoor and outdoor radio channels. The model for average large-scale path loss for arbitrary distances between TX and RX is expressed as a function of distance by using a path loss exponent, n, which indicates the rate at which the path loss increases with the distance. The log-distance path loss model is shown in (15) [Rap96, p.102].

$$L[dB] = 10 \cdot \log\left(\frac{P_{TX}}{P_{RX}}\right) = L(d_0) + 10 \cdot n \cdot \log\left(\frac{d}{d_0}\right) \quad (15)$$

where d_0 is the reference distance which is determined from measurements and d is the distance between TX and RX. The reference distance should be selected far enough and it should be in the far field of the antenna so that near-field effects do not affect the path loss. Typical reference distance for outdoor microcell systems is 100 meters. Typical path loss exponent values for different environments are shown in Table 1.

Table 1 Path loss exponents for different environments.

Environment	Path loss exponent, n
Free space	2
Urban area cellular radio	2.7 to 3.5
Shadowed urban cellular radio	3 to 5
Obstructed in building	4 to 6
Obstructed in factories	2 to 3

3.1.2. COST231 Walfisch-Ikegami model

The COST231 Walfisch-Ikegami (COST231 W-I in this paper) model gives more precise path-loss estimation than e.g. the COST231 Hata model. This is due to additional data parameters, which describe the characteristics of the environment: building heights h_{roof}, width of the roads w, building separation b and road orientation with respect to the direct radio path φ. The model distinguishes between LOS and NLOS situations. The path losses for both situations are given by the following equations [COS99, pp.136-139].

LOS-case:

$$L = 42.6 + 26 \log d_{[km]} + 20 \log f_{[MHz]} \quad (16)$$

NLOS-case is composed of the terms of free space loss L_0, roof-to-street diffraction and scatter loss L_{rts}, and multiple screen diffraction loss L_{msd}.

$$L = L_0 + L_{rts} + L_{msd} \quad (17)$$

$$L_0 = 32.5 + 20 \log d_{[km]} + 20 \log f_{[MHz]} \qquad (18)$$

$$L_{rts} = -16.9 - 10 \log w_{[m]} + 10 \log f_{[MHz]} + 20 \log \left(h_{roof} - h_{MS} \right) + L_{ori} \quad (19)$$

L_{ori} takes into account the street orientation:

$$L_{ori} = \begin{cases} -10 + 0.354\varphi, & 0° \leq \varphi \leq 35° \\ 2.5 + 0.075(\varphi - 35), & 35° \leq \varphi \leq 55° \\ 4.0 - 0.114(\varphi - 55), & 55° \leq \varphi \leq 90° \end{cases} \quad (20)$$

Multiple screen diffraction loss L_{msd} is calculated from the heights of buildings and their special separations along the radio path.

$$L_{msd} = L_{bsh} + k_a + k_d \log d_{[km]} + k_f \log f_{[MHz]} - 9 \log b_{[m]}$$
(21)

$$L_{bsh} = \begin{cases} -18 \log \left(1 + h_{BS} - h_{roof} \right), & h_{BS} \geq h_{roof} \\ 0, & h_{BS} \leq h_{roof} \end{cases} \quad (22)$$

$$k_a = \begin{cases} 54, & h_{BS} \geq h_{roof} \\ 54 - 0.8 \left(h_{BS} - h_{roof} \right), & h_{BS} \leq h_{roof}, d \geq 0.5km \\ 54 - 0.8 \left(h_{BS} - h_{roof} \right) \dfrac{d_{[km]}}{0.5}, & h_{BS} \leq h_{roof}, d \leq 0.5km \end{cases}$$
(23)

$$k_d = \begin{cases} 18, & h_{BS} \geq h_{roof} \\ 18 - 15 \dfrac{h_{BS} - h_{roof}}{h_{roof}}, & h_{BS} \leq h_{roof} \end{cases} \qquad (24)$$

$$k_f = \begin{cases} -4 + 0.7 \left(\dfrac{f_{[MHz]}}{925} - 1 \right), & \text{small cities} \\ -4 + 1.5 \left(\dfrac{f_{[MHz]}}{925} - 1 \right), & \text{large cities} \end{cases} \quad (25)$$

The term k_a represents the increase of the path loss for base station antennas below rooftops of the adjacent buildings. The terms k_d and k_f control the dependence of the multi-screen diffraction loss versus distance and radio frequency, respectively.

The following parameter ranges are allowed:

$$\begin{cases} d : 20m...5km \\ f = 800...2000MHz \\ h_{BS} = 4...50m \\ h_{MS} = 1...3m \end{cases} \qquad \begin{cases} w : 25m \\ h_{roof} : 20m \\ b : 200m \end{cases}$$

The COST231 W-I model is quite accurate for measurements of the base station height above rooftop level. However, the prediction error becomes large when the base station height approaches rooftop level. Furthermore, the performance of the model is poor when the base station heights are below rooftop level [COS99, p.139]. After the publication of the COST231 W-I model, its accuracy to predict the diffraction loss from the last rooftop to the street was questioned. Har states that the model predicts path loss 8.7 dB more optimistically than it is supposed to do. However, this error does not affect the path loss variations according to frequency, street width and building height [Har99b, p.1452].

3.1.3. Attenuation in vegetation (ITU-R P.833)

Attenuation in vegetation is dealt with in ITU-R Recommendation P.833, which provides a simple attenuation model for additional attenuation caused by vegetation in the frequency range 30 MHz – 60 GHz. In short-range outdoor radio communication systems attenuation in vegetation can play a significant role and it is important to take that into consideration. However, the wide range of conditions and types of foliage makes it difficult to develop a generalized prediction procedure. ITU-R P.833 introduces a general model of attenuation which is based on measurements.

Terrestrial path with one terminal in woodland

For a terrestrial radio path where one terminal is located within woodland, the additional loss due to vegetation can be characterised according to (26) [ITU03a, p. 1]:

$$A_{ev} = A_m \left(1 - e^{-\frac{d\gamma}{A_m}} \right), \qquad (26)$$

where d is the length of the path within woodland (m), γ is the specific attenuation for very short vegetative paths (dB/m) and A_m is the maximum attenuation for one terminal within a specific type and depth of vegetation (dB). Figure 5 [itu03a, p. 2] clarifies the situation. The excess attenuation A_{ev} is defined as excess to all other mechanisms, not just free space loss. Thus if the radio path geometry in Fig. 1 were such that full Fresnel clearance from the terrain did not exist, then A_{ev} would be the attenuation in excess of both free-space and diffraction loss.
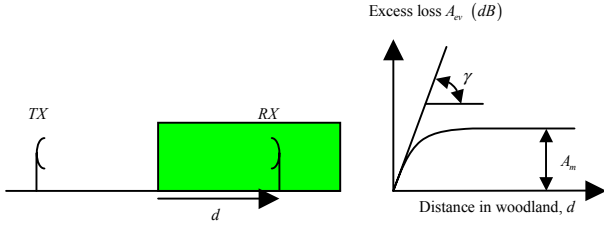
Figure 5 Representative radio path in woodland.

The value of γ depends on the species and density of the vegetation. Figure 6 [itu03a, p. 3] shows typical values for specific attenuation derived from various measurements over the frequency range 30 MHz to about 30 GHz in woodland. Below about 1 GHz there is a tendency for vertically polarized signals to experience higher attenuation than horizontally, due to scattering from tree-trunks.

The maximum attenuation A_m depends on the species and density of the vegetation, plus the antenna pattern of the terminal within the vegetation and the vertical distance between the antenna and the top of the vegetation.
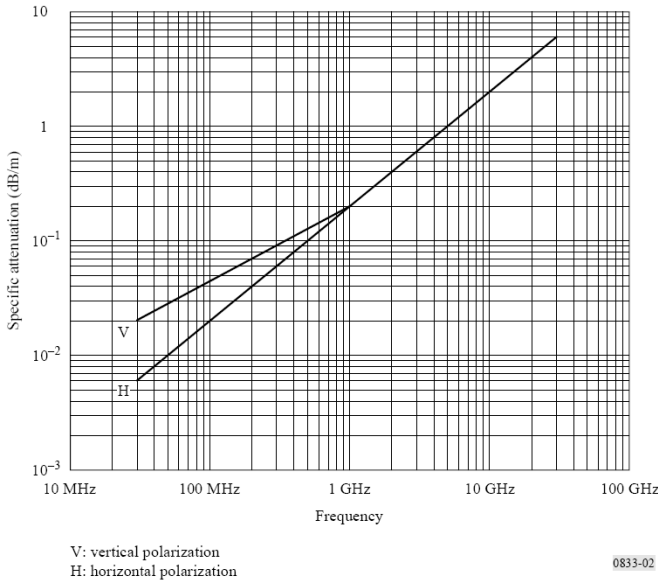

Figure 6 Specific attenuation due to woodland.

The frequency dependent equation of A_m (dB) can be seen in (27) [itu03a, p. 3].

$$A_m = A_1 f^{\alpha} \text{, where} \tag{27}$$

f is the frequency (MHz) used, A_1 and α are derived from the measurements:

- Measurements in the frequency range 900-1 800 MHz carried out in a park with tropical trees in Rio de Janeiro (Brazil) with a mean tree height of 15 m have yielded $A_1 = 0.18dB$ and

$\alpha = 0.752$. The receiving antenna height was 2.4 m. For example, an interpolation result at 2.4 GHz gives $A_m = 62.69dB$.

- Measurements in the frequency range 900-2 200 MHz carried out in a forest near Mulhouse (France) on paths varying in length from a few hundred metres to 6 km with various species of trees of mean height 15 m have yielded $A_1 = 1.15dB$ and $\alpha = 0.43$. The receiving antenna in woodland was a λ/4 monopole mounted on a vehicle at a height of 1.6 m and the transmitting antenna was a λ/2 dipole at a height of 25 m. The standard deviation of the measurements was 8.7 dB. Seasonal variations of 2 dB at 900 MHz and 8.5 dB at 2 200 MHz were observed. For example, an interpolation result at 2.4 GHz gives $A_m = 32.67dB$.

Single vegetative obstruction

Equation (26) does not apply for a radio path obstructed by a single vegetative obstruction where both terminals are outside the vegetative medium, such as a path passing through the canopy of a single tree. At VHF and UHF, where the specific attenuation has relatively low values, and particularly where the vegetative part of the radio path is relatively short, this situation can be modelled on an approximate basis in terms of the specific attenuation and a maximum limit to the total excess loss as shown in (28) [itu03a, p. 4].

$$A_{et} = d\gamma \tag{28}$$

$A_{et} \leq$ lowest excess attenuation for other paths (dB)

It is emphasised, that A_{et} is only an approximation. In general it will tend to overestimate the excess loss due to the vegetation.

3.1.4. Log-normal shadowing

The log-distance path loss model presented in Section 3.1.1 does not take into account the fact that there can be significant differences between the radio wave propagation channels of two locations that still have the same distance between TX and RX. This leads to the feature that measured signals are different than the average value given by (15). The difference between these measurements and given equation is random and log-normally distributed about the mean distant-dependent value, as shown in (29).

$$L[dB] = 10 \cdot \log\left(\frac{P_{TX}}{P_{RX}}\right) = L(d_0) + 10 \cdot n \cdot \log\left(\frac{d}{d_0}\right) + X_{\sigma} \tag{29}$$

X_{σ} is a zero-mean Gaussian distributed random variable (in dB), that describes the shadowing with a standard deviation σ (in dB).

3.2. Small-scale propagation models and multipath

Small-scale fading, or simply just fading, describes the rapid changes of the amplitude of radio waves over a short period of time or travelled distance. Multipath fading is caused by interference between multiple receptions of the same signal. The signal travels along different paths, and therefore is received at slightly different times. These multipath components combine at the receiver antenna to give a resulting signal that varies widely in amplitude, phase or polarisation. A common multipath environment is a city, where the multipath components can reflect, penetrate, diffract and scatter from various obstacles and surfaces as shown in Figure 7.
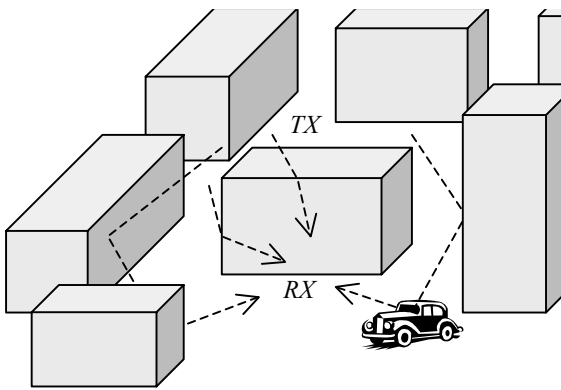

Figure 7 Multipath propagation in city environment.

Many methods have been developed to decrease the effect of multipath propagation. Usage of different diversity methods, e.g. space, time, frequency diversity etc., is a powerful method for reducing multipath fading. Multipath diversity means that multipath components are received in many different ways at the same time to increase the probability of receiving a strong signal at least in one way. For combining the received components, certain techniques, e.g. selection, equal-gain or maximum-ratio combining have been developed. More information about diversity can be found e.g. in [Rap96, p.325]. The RAKE receiver is also a commonly used countermeasure against the adverse effects of multipath propagation in spread spectrum systems like UMTS and WLAN. The RAKE receiver resolves the multipath structure of the channel using estimation, and equals the path delays. Then it performs combining of the signal components e.g. using maximum ratio combining. Also the uses of equalisers or smart antennas are powerful countermeasures against multipath fading.

In general, small-scale propagation channels are time and environment specific. These models require heavy measurement campaigns and the results are correct only for a given measurement location at the measurement instant. These channel models can be divided into narrowband and wideband channel

models. Narrowband models are simpler and their behaviour can be modelled with Rayleigh or Rice distribution functions. As the bandwidth increases a tapped delay line model is used with the individual tap amplitudes modelled with independent Rayleigh or Rice distributions. In very wideband channels new statistics of tap amplitude distribution are needed since Rayleigh and Rice distributions give poor models because of insufficient number of components.

3.2.1. Multipath propagation

The three most important effects of small-scale fading caused by multipath propagation and moving scatters are [Rap96, p.139]:

- rapid changes in signal strength over a small travelled distance or time interval,
- random frequency modulation due to varying Doppler shifts on different multipath signals, and
- time dispersion (echoes) caused by multipath propagation delays.

In city environments mobile radio system antenna heights are commonly well below the rooftop level of the surrounding buildings and therefore there might not be a line-of-sight path between TX and RX. Even if a LOS situation occurs there are many reflecting surfaces that still produce multipath components. Relative motion between TX and RX (or surrounding objects causing e.g. reflection) causes random frequency modulation, since each multipath component has a different Doppler shift. The Doppler shift can be calculated by using (30).

$$f_d = \frac{V}{\lambda}\cos\alpha, \qquad (30)$$

where V is the velocity of the terminal, α is the spatial angle between the direction of motion of the terminal and the direction of arrival of the wave, and λ is the wavelength.

3.2.2. System functions of the linear time-variant channel

The radio propagation channel can be visualised by a system element that transforms input the signal into an output signal. It is therefore similar to a linear filter with the extension that the radio propagation channel is time-variant. The radio channel can be modelled as a linear time-variant (LTV) channel that can be characterised by four functions, the time-variant impulse response (also known as the channel delay spread function [Bel63]), the time-variant transfer function, the channel output Doppler-spread function, and the delay/Doppler-spread function.

System functions of the deterministic LTV-channel

The time-variant impulse response $h(\tau, t)$ is shown in (31) [Par00, p.168].

$$h(\tau,t) = \sum_{n=1}^{N} h_n(t)\delta(\tau - \tau_n(t)), \qquad (31)$$

where $\tau_n(t)$ is the propagation delay of the nth propagation path as function of time and

$$h_n(t) = \alpha_n(t)e^{-j2\pi f_c \tau_n(t)}, \qquad (32)$$

where $\alpha_n(t)$ is the gain of the nth propagation path as function of time and f_c is the carrier frequency.

The time-variant transfer function is obtained by Fourier-transforming the impulse response with respect to the delay variable τ as shown in (33).

$$H(f,t) = F_\tau\{h(\tau,t)\} = \int_{-\infty}^{\infty} h(\tau,t)e^{-j2\pi f\tau}d\tau \quad (33)$$

The output Doppler-spread function is obtained by Fourier-transforming the time-variant transfer function with respect to the time variable t as shown in (34). It describes the channel frequency response to the frequency $f + v$.

$$D(f,v) = F_t\{H(f,t)\} = \int_{-\infty}^{\infty} H(f,t)e^{-j2\pi vt}dt$$

(34)

The delay/Doppler-spread function is obtained by Fourier-transforming the time-variant impulse response with respect to the time variable t as shown in (35), or by taking the inverse Fourier-transform of the output Doppler-spread function with respect to frequency. The delay/Doppler-spread function describes the complex gain of the channel in the delay interval $[\tau + d\tau]$ and the Doppler-shift interval $[v + dv]$.

$$S(\tau,v) = F_t\{h(\tau,t)\} = \int_{-\infty}^{\infty} h(\tau,t)e^{-j2\pi vt}dt \quad (35)$$

Figure 8 describes the relationships between the system functions. The relationships between system functions are assumed to be deterministic.
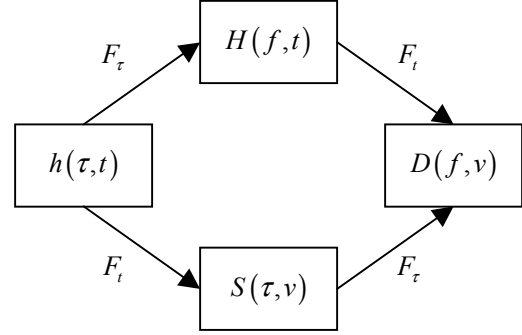

Figure 8 Relationships between deterministic system functions of an LTV-channel.

The characterisation of the system functions can then be extended to practical channels that are randomly time-variant. Wide-sense stationary uncorrelated scattering (WSSUS) channels are an important class of practical channels. More information of LTV-channels can be found e.g. in [Par00, pp.164-190] or in [Bel63].

System functions of the WSSUS random LTV-channel

A randomly time-variant LTV-channel is described using 4-dimensional autocorrelation functions that correspond to the previously described system functions. The use of these 4-dimensional autocorrelation functions is rather unpractical; two assumptions are made in order to get 2-dimensional autocorrelation functions [Pro95, p. 762]

- The LTV-channel under consideration is wide-sense stationary.

- The LTV-channel under consideration is a multipath channel where the propagation paths are statistically independent or at least uncorrelated.

This LTV-channel is called a WSSUS-channel (Wide-Sense Stationary Uncorrelated Scattering). The autocorrelation functions for a WSSUS-channel can be presented as $P_h(\tau,\Delta t), P_H(\Delta f,\Delta t), P_D(\Delta f,v)$ and $P_S(\tau,v)$ similarly as the previous system functions. The relationships between the autocorrelation functions are presented in Figure 9.

By putting one of the variables to zero, the following one-dimensional functions are obtained [Pro95, pp. 762-766]:

- The multipath intensity profile, also called power delay profile $P_h(\tau,0)$
- The frequency correlation function $P_H(\Delta f,0)$

- The time correlation function $P_H(0,\Delta t)$

- The Doppler power spectrum $P_D(0,v)$

Through these functions the characteristic parameters of the WSSUS channel, i.e. delay spread T_m,

coherence bandwidth B_m, coherence time T_D, and Doppler-spread B_D, can be obtained.

These multipath channel parameters are useful in order to compare different multipath channels. Delay spread quantifies the time dispersive properties of the channel, coherence bandwidth characterises the channel in frequency domain and Doppler Spread and coherence time describe the time varying nature of the channel.
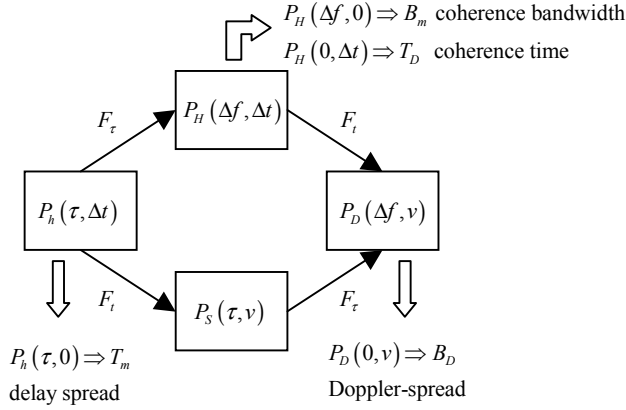

$P_H(\Delta f, 0) \Rightarrow B_m$ coherence bandwidth

$P_H(0, \Delta t) \Rightarrow T_D$ coherence time

$P_H(\Delta f, \Delta t)$

F_τ F_t

$P_h(\tau, \Delta t)$ $P_D(\Delta f, v)$

F_t $P_S(\tau, v)$ F_τ

$P_h(\tau, 0) \Rightarrow T_m$
delay spread

$P_D(0, v) \Rightarrow B_D$
Doppler-spread

Figure 9 Relationships between autocorrelation functions of a WSSUS channel.

The RMS (root mean square) delay spread S is the square root of the second central moment of the power delay profile (PDP) $P_h(\tau, 0)$ as shown in (36) [Par00, p.186].

$$S = \sqrt{\frac{\int_0^\infty (\tau - D)^2 P_h(\tau) d\tau}{\int_0^\infty P_h(\tau) d\tau}}, \qquad (36)$$

where D is the mean excess delay of the channel. It is the first moment of the power delay profile (PDP) as shown in (37) [Par00, p.186].

$$D = \sqrt{\frac{\int_0^\infty \tau P_h(\tau) d\tau}{\int_0^\infty P_h(\tau) d\tau}} \qquad (37)$$

The coherence bandwidth is a statistical measure of the range of frequencies over which the channel can be considered flat. It is defined as a range of frequencies over which two different frequency components have a strong possibility of amplitude correlation.

The Doppler spread B_D is a measure of the spectral broadening caused by the time rate of change of the mobile radio channel. It is defined as the range of

frequencies over which the received Doppler spectrum is essentially non-zero. If the baseband signal bandwidth is much greater than B_D, the effects of the Doppler spread are negligible at the receiver.

The coherence time T_D is the time domain dual of Doppler spread. It is used to characterise the time varying nature of the frequency dispersion of the channel in the time domain. The coherence time is actually a statistic measure of the time domain over which the channel impulse response is essentially invariant. The definition of coherence time implies that the channel affects differently to two signals arriving with a time separation greater than T_D.

3.2.3.   Types of small-scale fading

The type of fading depends on the nature of the transmitted signal with respect to the characteristics of the channel. The time dispersion and the frequency dispersion of the channel leads to four different types of fading that depend on the transmitted signal, the channel, and the velocity. While multipath delay spread leads to time dispersion and frequency selective fading, Doppler spread leads to frequency dispersion and time selective fading. The four types of fading are shown in Figure 10 [Rap96, p.166].
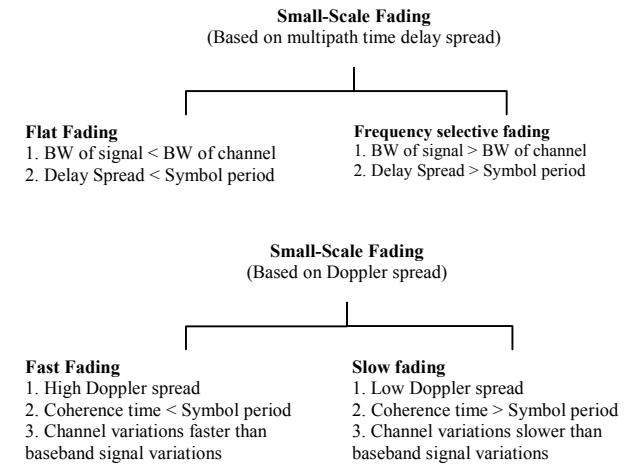

Small-Scale Fading
(Based on multipath time delay spread)

Flat Fading
1. BW of signal < BW of channel
2. Delay Spread < Symbol period

Frequency selective fading
1. BW of signal > BW of channel
2. Delay Spread > Symbol period

Small-Scale Fading
(Based on Doppler spread)

Fast Fading
1. High Doppler spread
2. Coherence time < Symbol period
3. Channel variations faster than baseband signal variations

Slow fading
1. Low Doppler spread
2. Coherence time > Symbol period
3. Channel variations slower than baseband signal variations

Figure 10 Types of small-scale fading.

Flat fading

The radio channel with constant gain and linear phase response over a bandwidth which is greater than the bandwidth of the transmitted signal, is called flat fading channel. In other words, flat fading occurs when the bandwidth of the transmitted signal is smaller than the coherence bandwidth of the channel, i.e. $B \ll B_m$. In such a channel, the effect can be seen as decrease of SNR (signal-to-noise ratio). Flat fading channels are also called amplitude varying channels or narrowband channels, since the bandwidth of the applied signal is narrow compared to the bandwidth of the flat fading channel.

11

Frequency selective fading

The radio channel with constant gain and linear phase response over a bandwidth which is smaller than the bandwidth of the transmitted signal, creates frequency selective fading in the channel. In other words, frequency fading occurs when the bandwidth of the transmitted signal is greater than the coherence bandwidth of the channel, i.e. $B >> B_m$. This means that different frequency components experience different kinds of attenuation and phase shifts in the channel and therefore can have different gains. Frequency selective fading also causes intersymbol interference (ISI). For frequency selective fading, the spectrum of the transmitted signal has a wider bandwidth than the coherence bandwidth of the channel. This type of fading can be caused by any delay difference between components and the fading increases as the delay spread increases. Frequency selective fading channels are also called wideband channels.

Fast fading

Fast fading occurs if the channel impulse response changes rapidly within the symbol duration. In other words, fast fading occurs when the coherence time of the channel is smaller than the symbol period of the transmitted signal, i.e. $T_D << T$. This causes frequency dispersion (also called time selective fading) due to Doppler spreading. Fast fading (as well as slow fading), deals with the rate of change of the channel due to motion.

Slow fading

Slow fading occurs when the channel impulse response changes at a rate much slower than the transmitted baseband signal. In other words, slow fading occurs when the coherence time of the channel is greater than the symbol period of the transmitted signal, i.e. $T_D >> T$. This means that the channel may be assumed static over one or several reciprocal bandwidth intervals. In the frequency domain the Doppler spread of the channel is much less than the bandwidth of the baseband signal.

The product of the delay spread and Doppler-spread $T_m B_D$ is called the spread factor of the channel. If $T_m B_D < 1$ the channel is said to be underspread; otherwise, it is overspread. For underspread channel it is possible to select the transmitted signal such that these channels are flat fading and slow fading [Pro95, p.771].

3.2.4. Distribution functions

In Section 3.1.4 the log-normal distribution was used to describe the large-scale shadow fading. For small-scale multipath components, the probability density function (PDF) is described by different statistical distribution functions. Rayleigh and Rice distributions can describe the PDF of the signal envelope changes in multipath situations with assumptions that the channel is flat fading and slow fading [Pro95, pp.772-773].

The Rayleigh distribution is commonly used to describe the statistical time varying nature of the received envelope of a flat fading signal, or the envelope of an individual multipath component [Rap96, p.172]. It is well known that the envelope of the sum of two quadrature Gaussian noise signals obeys the Rayleigh distribution. The PDF of the Rayleigh distribution is given by (38) [Rap96, p.172].

$$p(r) = \frac{r}{\sigma^2} e^{-\frac{r^2}{2\sigma^2}}, \left(0 \leq r \leq \infty\right) \qquad (38)$$

where σ^2 is the time-average power of the received signal before envelope detection, r is the Rayleigh fading signal envelope and $r^2/2$ is the instantaneous power.

In situations when a dominant stationary (nonfading) signal component, such as the line-of-sight component, exists in the channel, the small-scale fading envelope distribution is Ricean. The PDF of the Rice distribution is given by (39) [Rap96, p.176].

$$p(r) = \frac{r}{\sigma^2} e^{-\frac{(r^2 + A^2)}{2\sigma^2}} I_0 \left(\frac{Ar}{\sigma^2}\right) \left(A \geq 0, r \geq 0\right) (39)$$

where A is the dominant component of the signal and I_0 is the modified Bessel function of the first kind and zero order.

The Ricean distribution is often described by a parameter K, which is defined as the ratio between the deterministic signal power and the variance of the multipath, as shown in (40). K is called the Ricean factor.

$$K[dB] = 10 \log \left(\frac{A^2}{2\sigma^2}\right) \qquad (40)$$

When this dominant component exists ($A > 0$) the Ricean distribution is generated; whereas when the dominant component fades away (A approaches zero) the Ricean distribution degenerates to the Rayleigh distribution.

3.2.5. Tapped delay line channel model

As earlier mentioned, the Rayleigh and Rice distributions are not suitable for modelling the behaviour of a channel when the bandwidth of the channel increases. When a bandwidth $W >> B_m$ is available to the user, the wideband channel is generally characterised by the tapped delay line channel model. The channel is still assumed to be slowly fading, i.e. $T << T_D$. For a fixed number of taps, parameters

characterising the multipath behaviour, such as excess delay, normalised amplitudes and amplitude distributions, are calculated. The tapped delay line channel is represented by a time-variant FIR-filter in complex equivalent low-pass (ELP) signal domain. The tapped delay line model with K tap coefficients $h_k(t)$, $k = 0,1,...,K-1$ is shown in Figure 11 [Pro95, p.797].
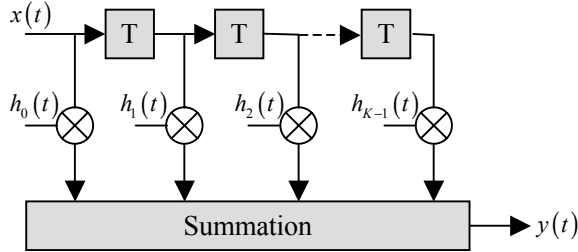

Figure 11 Tapped delay line presentation of a wideband multipath radio channel.

The channel input and output functions, $x(t)$ and $y(t)$ respectively, are generally complex. The unit tap delay of the model is denoted by T, which is an integer multiple of the simulation system sampling interval T_S, usually $T = T_S$ or $T = 1/W$ [Pro95, p.797], where W is the bandwidth occupied by the real bandpass signal.

Since the total multipath spread is T_m, for all purposes the tapped delay line model for the channel can be truncated at K taps according to (41) [Pro95, p.797].

$$K = (T_m W) + 1 \qquad (41)$$

The output function is given by (42).

$$y(t) = \sum_{k=1}^{K} x\left(t - \frac{k}{W}\right) h_k(t), \qquad (42)$$

The time-variant tap coefficients $h_k(t)$ are complex-valued stationary random processes. Since $h_k(t)$ represent the tap weights corresponding to the K different delays $\tau = k/W$, $k = 0,1,2,...,K-1$, the uncorrelated scattering assumption made in Section 3.2.2 implies that $h_k(t)$ are mutually uncorrelated [Pro95, p.797].

The tapped delay line model with only one tap represents the narrowband channel case, and as the bandwidth of the transmitted signal increases the number of taps increases also. In the special case of Rayleigh fading, the magnitudes of the taps are Rayleigh distributed and the phases are uniformly distributed [Pro95, p.797]. However, as the bandwidth increases even more, the Rayleigh or the Rice

distributions are no longer valid. In such a case also the number of taps can increase to give very impractical models. One possibility is to use sparse channel models, in which a large part of the tap coefficients are set to zero. This leads to the situation where the tap delays do not necessarily have to be uniformly distributed.

3.2.6. UMTS model

The development of UTMS in recent years has created the need for channel models for the 2 GHz frequency band. UTMS operates at a slightly lower centre frequency than WLAN and the modulation bandwidth of UTMS is smaller (5 MHz). Nevertheless, the propagation information of UTMS is also quite appropriate for 2.4 GHz WLAN systems, although the UMTS channel model might not be relevant as such.

ITU has published a recommendation concerning WCDMA channel models. The ITU Recommendation ITU-R M.1225 covers indoor office, outdoor-to-indoor and vehicular environments. The vehicular environment model and its channel impulse response model (based on the tapped delay line model) can be assumed relevant here. The number of taps, the time delay relative to the first tap, the average power relative to the strongest tap, and the Doppler spectrum of each tap characterize the model. For a majority of time the RMS delay spread is relatively small, but there are occasions with 'worst case' multipath characteristics that lead to a much larger RMS delay spread. These 'worst case' situations occur relatively infrequently, but they can have a major impact on system performance. To model this behavior of the channel, two multipath channels are defined: channel A is the low delay spread case that occurs frequently, channel B is the medium delay spread case that also occurs frequently. Channel A is expected to be encountered 40% of time, while for channel B the value is 55 % of time. Table 2 shows the tapped-delay-line parameters of the vehicular test environment with high antennas [ITU97, p.28].

Table 2 Tapped-delay-line parameters of the vehicular test environment.

Tap	Channel A		Channel B		Doppler spectrum
	Relative delay [ns]	Avg. power [dB]	Relative delay [ns]	Avg. power [dB]	
1	0	0	0	-2.5	Classic
2	310	-1.0	300	-0.0	Classic
3	710	-9.0	8900	-12.8	Classic
4	1090	-10.0	12900	-10.0	Classic
5	1730	-15.0	17100	-25.2	Classic
6	2510	-20.0	20000	-16.0	Classic

3.2.7. Multipath propagation of short-range outdoor radiocommunication (ITU-R P.1411)

Multipath propagation of short-range outdoor radiocommunication is also dealt within ITU-R

Recommendation P.1411, which introduces a general model for estimation of delay spread and number of signal components arriving at the receiver.

Estimation of delay spread

The recommendation covers characteristics of multipath delay spread for urban high-rise environment for microcells and picocells. The characteristics are based on measurement data at frequencies from 2.5 GHz to 15.75 GHz at distances from 50 to 400 m. The RMS delay spread S at distance d meters follows a normal distribution with the mean value D given by (43) and the standard deviation is given by (44) [itu03b, p. 14].

$$D = C_a d^{\gamma_a} \; [ns] \tag{43}$$

$$\sigma_S = C_\sigma d^{\gamma_\sigma} \; [ns], \tag{44}$$

where C_a, C_σ, γ_a and γ_σ depend on the antenna height and the propagation environment. Some typical values of coefficients for distances 50 to 400 m are listed in Table 3 [itu03b, p. 14].

Table 3 Typical coefficients for the distance characteristics of RMS delay spread.

Measurement conditions				D		σ_S	
Area	f (GHz)	h_b (m)	h_m (m)	Ca	γ_a	C_σ	γ_σ
Urban	2.5	6.0	3.0	55	0.27	12	0.32
	3.35-15.75	4.0	2.7	23	0.26	5.5	0.35
	3.35-8.45		1.6	10	0.51	6.1	0.39
			0.5				
Residential	3.35	4.0	2.7	2.1	0.53	0.54	0.77
	3.35-15.75		1.6	5.9	0.32	2.0	0.48

The average shape of the delay profile for 2.5 GHz in dB form can be seen in (45) [itu03b, p. 14].

$$P(t) = P_0 + 50 \left(e^{-\frac{t}{\tau}} - 1 \right), \tag{45}$$

where P_0 is the peak power (dB) and t is in ns. τ is the decay factor, which for LOS case can be estimated by (46).

$$\tau = S + 266 \tag{46}$$

Characteristics of multipath delay spread for both LOS and NLOS case in an urban high-rise environment for small macro-cells have been developed based on measured data at 1 920-1 980 MHz and 2 110-2 170 MHz using omni-directional antennas. The medium RMS delay spread S in this environment is given by (47) [itu03b, p. 15].

$$S_u = e^{(AL+B)} \tag{47}$$

where $A = 0.038$, $B = 2.3$ and L is path loss (dB).

Number of signal components

The number of signal components (i.e. a dominant component plus multipath components) can be identified from the delay profile as the number of peaks whose amplitudes are within A dB of the highest peak and above the noise floor.

Table 4 [itu03b, p. 17] shows the number of signal components for one scenario (a low BS antenna in a residential area). These figures are based on measurements and published in ITU-R P.1411-2. The temporal resolution in the measurements was 20 ns.

Table 4 Maximum number of signal components for a low BS antenna in an urban area.

Maximum number of components	A = 3 dB		A = 5 dB		A = 10 dB	
	80%	95%	80%	95%	80%	95%
	2	2	2	2	2	3
Freq (GHz)	3.35					
Antenna height (m)	4 (h_b)				2.7 (h_m)	
Range (m)	0-480					

Table 5 [itu03b, p. 17] shows the results of measurements for a high BS antenna in a suburban environment. The temporal resolution in these measurements was 50 ns. These tables list the maximum number of signal components which have been observed at 80% and 95% of locations in each measurement section.

Table 5 Maximum number of signal components for a high BS antenna in a suburban area.

Maximum number of components	A = 3 dB		A = 5 dB		A = 10 dB	
	80%	95%	80%	95%	80%	95%
	1	2	1	3	3	5
Freq (GHz)	3.67					
Antenna height (m)	40 (h_b)				2.7 (h_m)	
Range (m)	0-5000					

4. Summary

In this paper a brief overview of the WLAN channel modelling has been given. All channel models are based on four basic phenomenon of radio wave propagation; free space loss, reflection and penetration, diffraction and scattering. Channel models can be categorised in multiple ways. In this paper, distinction is made between large-scale and small-scale models.

The large-scale channel models are quite simple, and take into account only couple of parameters. These models are useful for coverage planning purposes. Large-scale fading models typically include path loss over distance and shadowing models

The small-scale radio channel can be modelled as a linear time-variant (LTV) channel that can be characterised by four functions, the time-variant impulse response (also known as the channel delay

spread function [Bel63]), the time-variant transfer function, the channel output Doppler-spread function, and the delay/Doppler-spread function.

In this paper some typical large-scale and small-scale models are presented. Presented models are suitable for WLAN systems at 2.4 GHz frequency band.

5. References

[Ame53] W.S. Ament, "Toward a theory of reflection by a rough surface", *Proceedings of the IRE*, Vol. 41, No. 1, January 1953, pp. 142-146

[Bel63] P.A. Bello, "Characterization of randomly time-variant linear channels", *IEEE Trans.*, Vol CS-11, No 4, December 1963, pp. 360-393

[COS99] COST Action 231E Final Report, *"Digital mobile radio towards future generation systems"*, ISBN 92-828-5416-7, European Communities, Belgium, 474 pp., 1999

[Har99a] D. Har, H.H. Xia, H.L. Bertoni, "Path-Loss Prediction Model for Microcells", *IEEE Transactions on Vehicular Technology*, vol. 48, no. 5, September 1999, pp. 1453-1462

[Har99b] D. Har, A.M. Watson, A.G. Chadney, "Comment of Diffraction Loss of Rooftop-to-Street in COST231-Walfisch-Ikegami Model", *IEEE Transactions on Vehicular Technology*, Vol 48, No 5, September 1999, pp. 1451-1452

[ITU97] ITU-R Recommendation M.1225, *"Guidelines for valuation of radio transmission technologies for IMT-2000"*, ITU-R, 60 pp., 1997

[ITU03a] ITU-R Recommendation P.833-4, *"Attenuation in vegetation"*, ITU-R, 7 pp., 2003

[ITU03b] ITU-R Recommendation P.1411-2, *"Propagation data and prediction methods for the planning of short-range outdoor radiocommunication systems and radio local area networks in the frequency range 300 MHz to 100 GHz"*, ITU-R, 17 pp., 2003

[Lin96] I. Lindell, *"Radioaaltojen eteminen (Radio wave propagation, in Finnish)"*, ISBN 951-672-227-X, 4th ed., Otatieto Oy, Helsinki, 261 pp., 1996

[Nik92] K. Nikoskinen, *"Sähkömagnetiikan kaavoja (Equations for electromagnetism, in Finnish)"*, ISBN 951-672-142-7, Otatieto Oy, Helsinki, 124 pp., 1992

[Par00] J.D. Parsons, *"The mobile radio propagation channel"*, 2nd edition, ISBN 0-471-98857-X, Wiley, London, 418 pp., 2000

[Pro95] J.G. Proakis, *"Digital Communications"*, 3rd edition, ISBN 0-07-113814-5, McGraw-Hill Book Co., Singapore, 928 pp., 1995

[Rap96] T.S. Rappaport, *"Wireless Communications"*, ISBN 0-13-461088-1, Upper Saddle River (NJ), Prentice Hall PTR, 641 pp., 1996

Homework

Additional information might be needed.

1) Calculate received signal strength in a situation that IEEE 802.11b WLAN base station is located in a small European city environment and the receiving mobile station is located in the private house nearby. MS uses an outside antenna with 3 dB gain. MS antenna height is 3m. Between base station and mobile station there is a small park (width 25m) with tall trees, and the house is located very close to the other edge of the park, but it is assumed to be inside the park. Average height of the building in the city is 20m, building separation is 200m and street width is 20m. Base station antenna height is 10m. Distance between RX and TX is assumed 60m. Base station uses maximum allowed EIRP power. Roads are orientated 25° away from the direction of the BS.

2) Is it possible to use the system?